A Serpentinite-Hosted Ecosystem: The Lost City Hydrothermal Field

Deborah S. Kelley,[1]* Jeffrey A. Karson,[2] Gretchen L. Früh-Green,[3] Dana R. Yoerger,[4] Timothy M. Shank,[4] David A. Butterfield,[5] John M. Hayes,[4] Matthew O. Schrenk,[1] Eric J. Olson,[1] Giora Proskurowski,[1] Mike Jakuba,[6] Al Bradley,[4] Ben Larson,[1] Kristin Ludwig,[1] Deborah Glickson,[1] Kate Buckman,[4] Alexander S. Bradley,[7] William J. Brazelton,[1] Kevin Roe,[5] Mitch J. Elend,[1] Adélie Delacour,[3] Stefano M. Bernasconi,[3] Marvin D. Lilley,[1] John A. Baross,[1] Roger E. Summons,[7] Sean P. Sylva[4]

The serpentinite-hosted Lost City hydrothermal field is a remarkable submarine ecosystem in which geological, chemical, and biological processes are intimately interlinked. Reactions between seawater and upper mantle peridotite produce methane- and hydrogen-rich fluids, with temperatures ranging from <40° to 90°C at pH 9 to 11, and carbonate chimneys 30 to 60 meters tall. A low diversity of microorganisms related to methane-cycling Archaea thrive in the warm porous interiors of the edifices. Macrofaunal communities show a degree of species diversity at least as high as that of black smoker vent sites along the Mid-Atlantic Ridge, but they lack the high biomasses of chemosynthetic organisms that are typical of volcanically driven systems.

In 1979, the world was astounded by the discovery of hydrothermal chimneys and black smoker vents driven by the cooling of magma beneath mid-ocean ridges and hosting oases rich in chemosynthetically based biological communities (*1*). Since that pivotal find, more than 200 vent fields have been documented in the ocean basins (*2*). The associated metal deposits and diverse biota of clams, tubeworms, and swarming shrimp have become the familiar hallmarks of submarine hydrothermal vent systems. Many of these high-temperature systems are restricted to the axis of the global mid-ocean ridge spreading network, where more than 85% of Earth's magmatic output is localized (*3*). This localization has led researchers to focus on an extremely narrow corridor (<1 to 5 km wide) along the axis of the ridge.

In 2000, a hydrothermal field called Lost City was serendipitously discovered more than 15 km away from the spreading axis of the Mid-Atlantic Ridge (MAR) at a water depth of 750 to 900 m (Fig. 1). Initial studies based on a single dive by the deep submergence vehicle *Alvin* showed that it was unlike any hydrothermal system found to date, hosting diffusely venting carbonate monoliths towering tens of meters above the seafloor (*4*). The composition of its fluids derives from reactions between seawater and uplifted mantle peridotite rather than from interactions between seawater and cooling basalts (*4*). Subsurface, exothermic, mineral-fluid reactions associated with the oxidation of iron in cooling mantle peridotite produce alkaline fluids rich in hydrogen and methane at venting temperatures up to 90°C (*4*, *5*). These high-pH volatile-rich fluids trigger carbonate precipitation upon mixing with seawater and serve as important energy sources for microorganisms that thrive in the porous chimney walls.

These peridotite-hosted biotopes differ substantially from axial, magmatically driven vent systems in which carbon dioxide and hydrogen sulfide are the dominant volatile species (*5*, *6*). Exposed serpentinized peridotites are widespread (*7*–*10*), and reactions similar to those producing the Lost City hydrothermal field (LCHF) are probably common in these areas, implying that there may be extensive unexplored regions of the ocean basins harboring life forms that are not solely supported by magmatically driven hydrothermal flow. In addition, peridotite-hosted systems can be long-lived: ^{14}C dating shows that hydrothermal activity at Lost City has been ongoing for at least 30,000 years (*11*). Modeling of this system suggests that hydrothermal activity sustained by serpen-

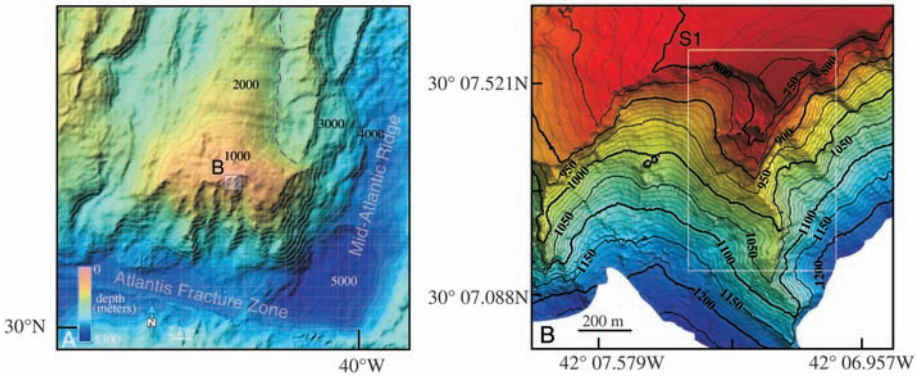

Fig. 1. (**A**) The Atlantis massif is located ~15 km to the west of the MAR axial valley. The intersection of the Atlantis Fracture Zone and the MAR is marked by a ~6000-m-deep nodal basin. Within a horizontal distance of ~20 km, the seafloor rises to within 700 m of the surface. On the basis of magnetic data, the massif has been uplifted at rates comparable to those of the Himalayan mountains (*15*). Well-developed corrugations on the surface of the massif are believed to be traces of a long-lived detachment fault that dips gently beneath the axis of the MAR (*15*). The flat elongate bench on the eastern side of the massif is interpreted as the hanging wall of the fault and is composed of volcanic material. Lost City is located within the small box near the central summit of the massif. (**B**) Shaded bathymetric map based on *ABE* data for the LCHF and adjacent terrain. Most of the small mound-shaped structures are individual chimneys or clusters of carbonate chimneys that delineate an east-west trend that marks a major lineament. A zone of continuous carbonate composed of multiple edifices forms the core of the field. It extends nearly 200 m in length and several tens of meters down the cliff face to the south. Hydrothermal fluids are weeping actively from many of these steep cliffs. S1, fig. S1.

[1]School of Oceanography, University of Washington, Seattle, WA 98195, USA. [2]Division of Earth and Ocean Sciences, Duke University, Durham, NC 27708, USA. [3]Department of Earth Sciences, ETH-Zentrum, Zurich, Switzerland. [4]Woods Hole Oceanographic Institution (WHOI), Woods Hole, MA 02543, USA. [5]Joint Institute for the Study of the Atmosphere and Ocean, University of Washington, and National Oceanic and Atmospheric Administration Pacific Marine Environmental Laboratory, Seattle WA 98115, USA. [6]MIT/WHOI Joint Program, WHOI, Woods Hole MA 02543, USA. [7]Department of Earth, Atmospheric, and Planetary Sciences, Massachusetts Institute of Technology, Cambridge MA 02139, USA.

*To whom correspondence should be addressed. E-mail: kelley@ocean.washington.edu

tinization reactions may last for hundreds of thousands of years (*11*, *12*). Alkaline systems such as the LCHF may have been characteristic of early Earth hydrothermal environments, where the eruption of Mg-rich komatiitic lavas was common (*13*).

In 2003, a second expedition returned to the LCHF to study the linkages between hydrothermal alteration of mantle peridotite, fluid geochemistry, and biological activity. The field program included 19 dives with the submersible *Alvin* and an unconventional mapping effort with the *Autonomous Benthic Explorer* (*ABE*) in this area of extreme topography (*14*). Ten discrete active vent sites were sampled for the first time for co-registered fluids, rocks, and biota (Figs. 1 and 2 and fig. S1). Here we present an integrated summary of our field studies and laboratory findings. Our results provide a comprehensive overview of the geological and structural controls on fluid flow at Lost City and elucidate the consequences of fluid/rock interaction in the basement for fluid chemistry and chimney growth and for the life that can be supported in these environments.

Geologic setting. The *Alvin* and *ABE* surveys delineate the southern scarp of the massif and the major fault lineaments that intersect it (Figs. 1B and 2 and fig. S1). Variably foliated serpentinite, talc-amphibole schist, and metagabbroic rocks make up the nearly continuous cliffs at the top of the scarps to the northwest and northeast of the LCHF. Near the summit of the massif, we identified a ~50-m-thick mylonitic-to-cataclastic shear zone that includes lenses of less deformed material (Fig. 3 and fig. S1). This shear zone is probably the long-lived detachment fault that exposed the mantle and lower crustal rock sequences that make up the massif (*15*). This zone grades downward into massive jointed rocks that lack a strong deformation fabric. The basement rocks in the vicinity of the field are cut by veins of calcite and aragonite, which derive from some of the oldest hydrothermal activity at this site (*11*).

The summit of the massif is capped by 1 to 3 m of flat-lying sedimentary breccias overlain by variably lithified, fossiliferous pelagic limestone with sparse bedrock clasts. The breccias probably represent debris slide deposits shed onto the sloping detachment fault surface when it defined the median valley wall. As that surface moved off axis and flattened into its present subhorizontal orientation, the sedimentary regime changed from clastic to pelagic. Exiting high-pH hydrothermal fluids generated by serpentinization probably enhanced carbonate precipitation and cementation of these sediments (*16*). The resulting cap rock was important in the formation of the LCHF, acting as an impervious lid trapping both fluids and heat.

The LCHF. The LCHF lies atop the sedimentary cap rock, on a triangular down-dropped block that forms a terrace on the edge of the south wall (Figs. 1B and 3). Our mapping indicates that the largest and most active vents are along an east-west trending lineament more than 300 m long (Fig. 1B and fig. S1). The lineament is intersected by a fault trending approximately north-south, which exposes massive jointed outcrops of relatively undeformed serpentinized harzburgites that form the major north-south ridge just south of the field. Toward the top of the scarp, these rocks are strongly foliated and are overlain by the sedimentary cap rocks. This distinctive surface is seen in the higher scarps to the northeast and northwest. The difference in depth between equivalent outcrops indicates that there has been at least 150 m of vertical displacement on a fault that trends west-northwest. This fault and faults with similar trends are essentially parallel to the nearby Atlantis Transform fault. Transform-parallel faults with extensive vertical offsets are typical of many other oceanic massifs (*7*, *17*).

The fracture and fault network in the basement provides permeable pathways that control outflow at the main vent sites. In addition to the subvertical faults that channel flow to the largest structures, much of the subsurface flow emanates from surfaces that are parallel to basement foliation and subparallel to gently west-dipping faults (Fig. 3). The steep faults expose relatively old inactive stockworks

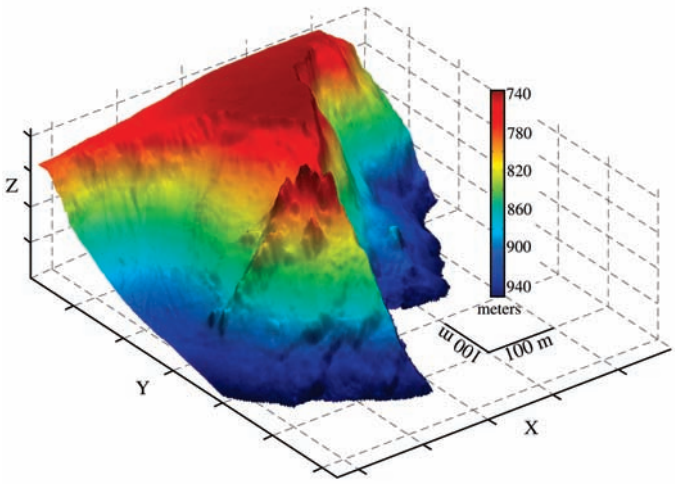

Fig. 2. Three-dimensional view, looking toward the northeast, of the LCHF. This image is based on 17 *ABE* missions using the SM2000 sonar system in a down-looking and side-looking mode. The LCHF is in the foreground; at depths less than ~900 m, the area is characterized by nearly continuous carbonate chimneys, spires, and debris. The massive pinnacles at the summit of this platform are the composite, actively venting edifices that make up the massive 60-m-tall structure called Poseidon. The area is characterized by extreme topographic relief, with vertical-to-subvertical cliffs and overhanging ledges in the serpentinite bedrock. The smooth surface in the background is the summit of the Atlantis massif.

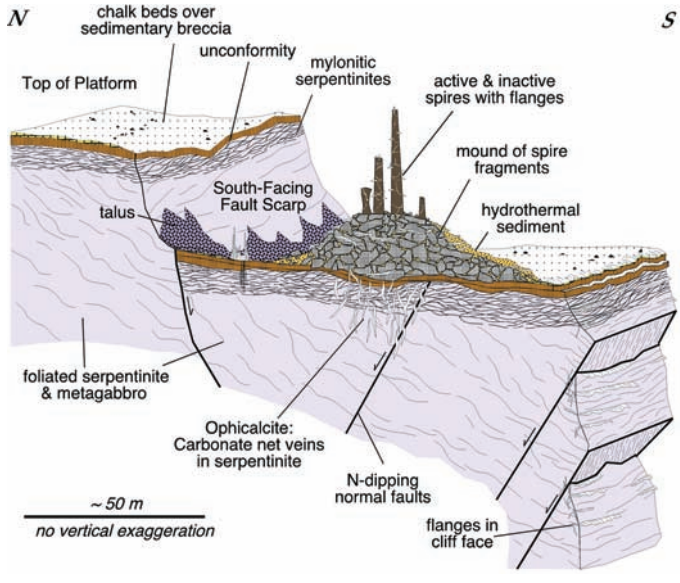

Fig. 3. Diagrammatic sketch showing geologic and tectonic relationships at Lost City. Hydrothermal structures are located on a faulted down-dropped block of variably altered and deformed crust composed predominantly of serpentinite. It is likely that hydrothermal flow is focused by intersecting fractures associated with transform fault development and uplift of the massif. In addition, an up to 40% increase in rock volume resulting from serpentinization may enhance fracturing, significant mass wasting (in a manner analogous to subaerial frost action), and hydrothermal flow. The networks of carbonate veins and carbonate cemented breccias associated with this field are very similar to ophicalcite deposits found in Alpine ophiolites and in other more ancient ophiolites.

of carbonate veins and subhorizontal-to-subvertical open fractures in the basement rock. These are actively leaking hydrothermal fluid and feeding young white hydrothermal precipitates (Fig. 4).

The white hydrothermal deposits range from arrays of delicate fingerlike crystals to beehivelike masses that are a few tens of centimeters across, growing directly out of cracks (Fig. 4E). Individual conduits are sealed by growths of calcium carbonate. Overgrowths and swaths of younger carbonate cutting across older material suggest reactivation and multiple stages of fracturing. Control of the hydrothermal outflow by fractures is particularly obvious where walls of massive shingled carbonate have been deposited on the steep scarps, highlighting the fact that much of the LCHF plumbing system is in marked contrast to the vertical conduits that typify black smoker environments and continental sulfide deposits.

The core of the field is dominated by the actively venting carbonate monolith called Poseidon (fig. S1), an edifice that rises >60 m above the seafloor (~800 m of water depth). This composite structure is composed of four large columns that are several meters in diameter (Figs. 2 and 4B). These pinnacles coalesce at their base to form a massive east-west trending structure extending at least 50 m. Parasitic chimneys, resembling inverted stalactites, are particularly abundant on the northwest face, as are actively venting flanges, or ledges that protrude several meters from the main trunk (Fig. 4C).

The most visually striking region is just northeast of Poseidon, in an area about 70 m in length at a water depth of 800 to 900 m (markers 7 and H, fig. S1). In this area, the vertical serpentinite cliffs are draped with deposits that have astoundingly diverse morphologies. Fluids weeping from the scarp face have produced clusters of delicate multipronged carbonate growths that extend outward like the fingers of upturned hands. Multipinnacled chimneys, some reaching 10 m in height, grow vertically out of the cliff faces (Fig. 4A), and single chimneys that sprout from more gently dipping bedrock reach 30 m in height (Fig. 4D and movie S1). These structures form a nearly continuous carbonate deposit that can be traced for over 200 m in length along the 850- to 900-m contour (fig. S1).

The northern portion of the field is bounded by a shallow depression (Fig. 1B) that is closed to the east and gradually deepens to the west. Nicknamed ''Chaff Beach'' (fig. S1), this gently sloping area is covered by variably cemented foraminifera, pteropod shells, coral debris, urchin spines, and hydrothermally derived carbonate crust. Concentrations of CH_4 in the water column here are 30 times (55 nM) those in background ocean water at depths ~50 m above the seafloor [supporting online material (SOM) text and fig. S1]. Hydrogen concentrations are over 100 times (349 nM) those of background seawater values. This ground fog of volatile-enriched fluids may represent the leaking of diffuse alkaline fluids through the underlying serpentinites, leading to rapid lithification of the pelagic sediments. Hydrocasts conducted ~75 to 100 m east of the main field also detected volatile enrichment up to 150 m above the seafloor; the highest concentrations of CH_4 were measured here, reaching values of 180 nM.

Carbonate fluid chemistry. Geochemical and petrologic analyses of the carbonate rocks reveal distinct differences between the active and extinct structures. Actively venting chimneys and flanges are highly porous, friable formations composed predominantly of aragonite and brucite (Fig. 5). Brucite commonly encloses dendritic feathery growths of aragonite, showing that it is a later phase probably formed through mixing of magnesium-rich seawater and hydrothermal fluid. Distinct annular orifices, which are common in black smoker systems, are rare at Lost City. Instead, fluids emerge from complex networks of centimeter-sized channels. Petrographic analyses of the carbonate chimneys show fine anastomosing networks of carbonate lined with brucite, indicating mixing of seawater and hydrothermal fluids within the interior walls.

In contrast to the active structures, extinct chimneys are less porous, well lithified, and have a higher abundance of calcite. Prolonged lower-temperature interactions with seawater

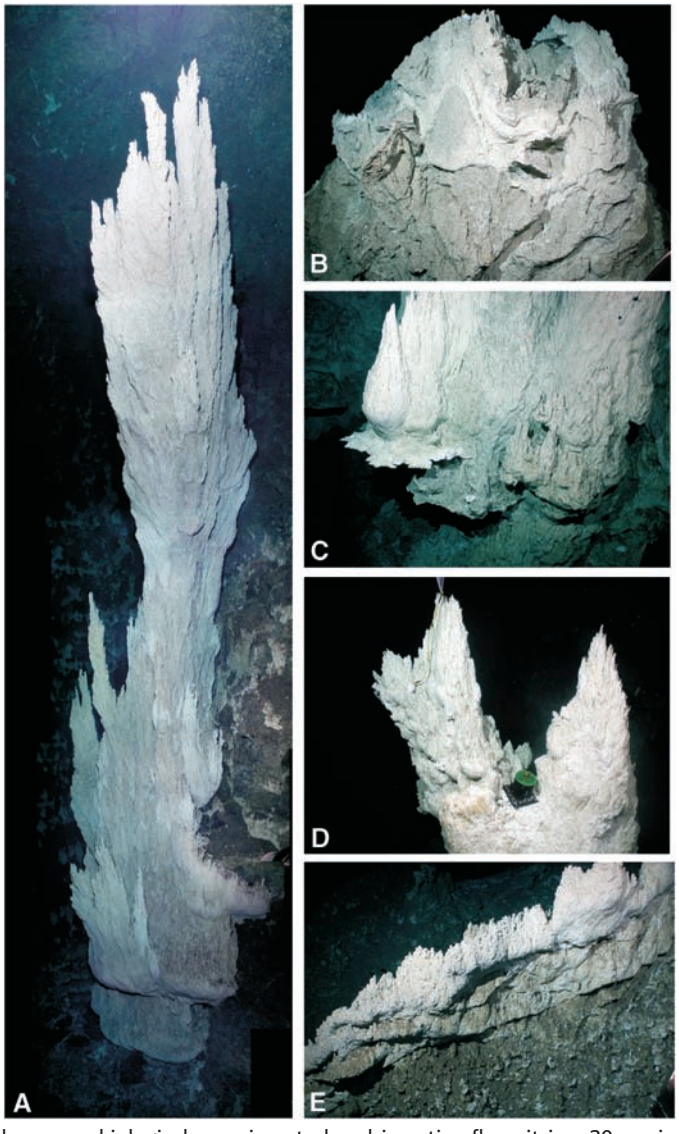

Fig. 4. Hydrothermal deposits at Lost City. (**A**) Graceful, 10-m-tall, actively venting carbonate chimney growing directly out of a serpentinite cliff on the eastern side of the field. The small carbonate deposits in the background mark sites of active and inactive seeps along the steep walls. (**B**) One of four actively venting peaks that make up the massive hydrothermal structure called Poseidon. Young and/or actively venting material is white in color; inactive areas are brown to cream-colored. This pinnacle is ~4 m across. (**C**) The base of the "IMAX" flange, which is a three-story-tall spirelike growth on the side of Poseidon. This area is actively venting 55°C fluids that support dense microbial communities. (**D**) Actively venting 50°C pinnacle on the east side of the field, showing young feathery growths of carbonate. This edifice is growing in a large vertical crevice within the wall. Actively venting carbonate flanges, which are several meters across, form overhanging ledges above and to the sides of the chimney. The green-capped black cylinder at the notch between the two pinnacles was a biological experiment placed in active flow; it is ~20 cm in diameter. (**E**) Feathery carbonate growth rising from a vein within the serpentinite bedrock. Many of these veins are several centimeters across. Near the summit of the massif they form dense cross-cutting networks that mark fossilized stockwork systems, which fed past sites of venting.

and hydrothermal fluids within the chimneys result in the conversion of aragonite to calcite, the enrichment of some trace metals (such as Mn, Sr, and Ti), and the dissolution of brucite (SOM text). They also promote the incorporation of foraminifera within the outer cemented walls of the carbonate structures. Mineralogical transformations are reflected in the bulk rock chemistry of the structures. The most active structures contain up to 27 weight % (wt %) Mg and down to 5 wt % Ca, whereas the extinct structures contain as little as <1 wt % Mg and up to 36 wt % Ca. Changes in strontium isotopic compositions accompany these transformations, with the youngest active samples yielding mantle-influenced $^{87}Sr/^{86}Sr$ values of 0.7076 to 0.7079. Inactive samples yield ratios of up to 0.7090, which is near that of seawater (*11*).

Analyses of stable isotopes in >50 vent and fissure-filling carbonates sampled in 2000 and 2003 yielded highly variable carbon and oxygen isotope compositions (SOM text). Although >70% of the samples have $\delta^{13}C$ values close to marine values within 2 per mil (‰) of 0 versus Vienna Pee Dee belemnite (VPDB) values, the range extends from –7 to +13‰. The oxygen isotope compositions vary from –7 to +5‰ (VPDB). A large number of samples have $\delta^{18}O$ values >2‰ and probably reflect enrichment in ^{18}O during fluid/rock interaction, either within the vent structures or in the basement. Discrete carbonate veins and bulk carbonate in the basement have $\delta^{13}C$ values of –6 to +3.5‰ and $\delta^{18}O$ values down to –19‰. Large differences occur within single samples and at different locations, but the greatest variations are in vent samples with abundant brucite. This variability suggests that fluid compositions, temperatures, and microbial activity fluctuate geographically as well as through time.

The LCHF provides a rare example of seawater interacting directly with peridotite exposed on the seafloor. The chemistry of the fluids (and vent structures) is controlled by relatively low-temperature (<~150°C) reactions between seawater and peridotite beneath the Atlantis massif. The hottest samples collected from Poseidon (91°C) have Mg concentrations of <1 mmol/kg, verifying that a zero-Mg end member is produced in the serpentinization reaction zone (SOM text). Oxygen isotopic compositions of vent waters ($0.2 \leq \delta^{18}O \leq 0.7$‰ Vienna standard mean ocean water) increase linearly with temperature and depletion of Mg. Concentrations of sulfate in the hydrothermal end members are 1 to 4 mmol/kg. Significantly lower values would be expected if anhydrite were being precipitated. Accordingly, fluid temperatures within the massif under Lost City currently must be less than 150°C. The measured venting temperatures overlap with temperatures calculated from $\delta^{18}O$ analyses of the chimneys but are lower than those recorded in some basement samples, which locally indicate paleotemperatures up to ~185°C (*11*).

In the high-pH (10 to 11) end-member fluids, carbonate ion (CO_3^{2-}) is the dominant form of dissolved inorganic carbon (DIC), and carbonate alkalinity is less than one-third of seawater values, whereas calcium concentrations are elevated (up to 30 mmol/kg). Carbon dioxide normally contributed by magmatic sources at mid-ocean ridges is absent in the LCHF fluids (*5*, *18*). Thus, autotrophic organisms living in vents must be adapted to a low-DIC, CO_2-poor, and H_2-rich environment.

Isotopic compositions ($\delta^{13}C$) of DIC in the fluids range from –8 to –2‰ in low-sulfate end-member fluids and –1 to +3‰ in samples with sulfate concentrations closer to those of seawater (SOM text). S-isotope compositions of sulfate ($\delta^{34}S$) range from +30‰ (Vienna Canyon Diablo troilite) in the end-member fluids to +21‰ in those fluids with higher sulfate concentrations (SOM text). Although we consider the $\delta^{13}C$ (DIC) values to be minimum estimates (SOM text), the observed compositions are consistent with those of the vent carbonates and reflect the ^{13}C-enriched nature of carbon components in the LCHF system. This covariance suggests local sulfate reduction in the vent structures and/or in the shallow subsurface.

Methane concentrations are elevated relative to seawater, but fall within a narrow range between 1 and 2 mmol/kg. In contrast, hydrogen concentrations vary from <1 to 15 mmol/kg, spanning the range for nearly all vents measured along the global mid-ocean ridge system (*5*, *18*, *19*). The extreme enrichment of hydrogen with lesser methane is characteristic of fluids formed through serpentinization reactions (*20*–*24*). Methane of the LCHF fluids has high $\delta^{13}C$ values of –13.6‰ to –8.8‰ VPDB. These compositions are 5 to 10‰ enriched relative to CH_4 from East Pacific Rise and southern Juan de Fuca fluids (*25*–*27*), but are similar to CH_4 sampled near ultramafic sequences of the Oman ophiolite (*28*). They are slightly depleted (2 to 6‰) relative to CH_4 at the Zambales ophiolite (*29*). As discussed in detail below, a determination of the CH_4 source cannot be made from the stable isotope data alone.

Life in high-pH systems. The metabolic menu for autotrophic microbes at hydrothermal vents is defined by the fluid chemistry. In this respect, the LCHF offers markedly different fare from that at magmatically hosted sites on ridge axes. Hydrogen is the dominant reduced product of serpentinization reactions beneath the massif, and it is also the most abundant energy source for microbes. Methane is also found in these vent fluids. Together, H_2 and CH_4 account for more reducing power at the LCHF than sulfide, which is the most abundant reduced product in solution at hydrothermal sites associated with basaltic volcanism (*18*). Concentrations of dissolved metals are much lower at the LCHF, and the suite of hydrothermal precipitates is completely different from that at typical sulfide-hosted mid-ocean ridge vent sites. These differences are reflected by the distinct microbial communities found within

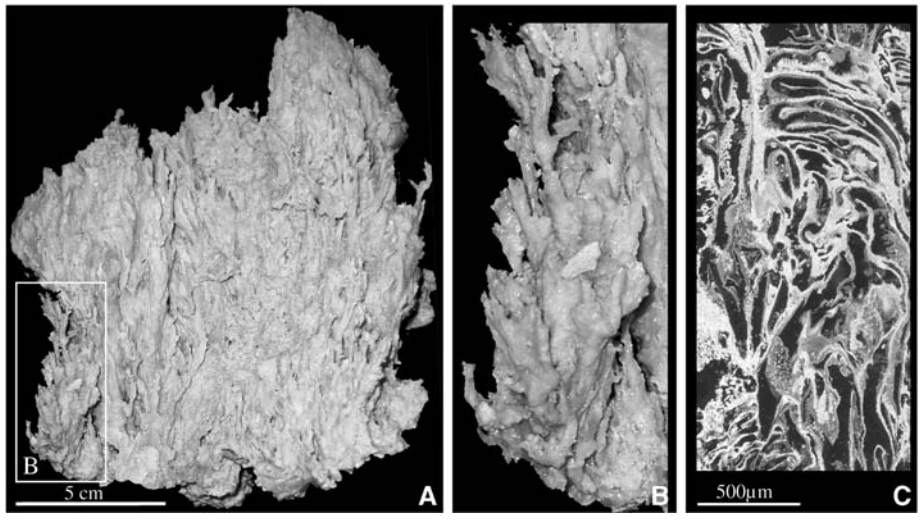

Fig. 5. Active vent deposits from Lost City. (**A**) Aragonite-rich sample recovered from near the summit of Poseidon. The sample was bathed in 59°C hydrothermal fluids. (**B**) Closeup of sample shown in (A), highlighting characteristic fragile intergrowths of aragonite and brucite. Carbonate chimneys and vein material in areas of active venting are snow white in color, extremely friable, and very porous. (**C**) Photomicrograph showing anastomosing aragonite intergrowths that are reminiscent of filamentous bacteria present in areas of diffuse flow (movie S2). This sample was recovered from a several-centimeter-wide "artery" of carbonate cutting the massif flanks of Poseidon. Feathery growths of carbonate several centimeters long protrude from the vein in a similar fashion to the deposit shown in Fig. 4E.

carbonate samples in contact with the warm high-pH hydrothermal fluids (*30*) (movie S2).

A suite of >60 active and inactive carbonate structures and venting hydrothermal fluids collected during the 2000 and 2003 cruises to the LCHF were investigated to quantify the numbers of microorganisms and their phylogenetic diversity (Table 1, Fig. 6, fig. S2, and SOM text). A range of biotopes harboring distinct microbial communities appear to be present at the LCHF. Carbonate samples in contact with active venting of warm volatile-rich hydrothermal fluids consistently harbored large numbers of microbes, nearly 10^7 to 10^8 cells per gram of wet weight (gww) (Table 1). In contrast, there were lower densities (<10^7 gww) in extinct samples (Table 1).

Overall, 29 to 57% of the cell population associated within active hydrothermal venting was counted by fluorescence in situ hybridization (FISH), and all of the higher-temperature (>50°C) samples yielded a higher proportion of archaea than bacteria. These results confirm our initial findings on a limited number of carbonate samples from the 2000 cruise, which showed the predominance of a single phylotype related to the archaeal order Methanosarcinales in spatially distinct sites on the Poseidon edifice (SOM text) (*30*). Between 70 and >90% of the archaeal cells in all of the higher-temperature samples hybridized with an oligonucleotide probe targeting this phylotype (Table 1) (*30*). The more recent samples support this conclusion and further suggest that both methane-producing and methane-consuming Archaea are present, on the basis of analyses of the *mcrA* (Fig. 6) and 16*S* ribosomal RNA (rRNA) genes (fig. S2). Our analyses indicate that the methanosarcinal phylotype found at the LCHF appears to be associated with carbonate-hosted environments in contact with higher-temperature end-member fluids. In contrast, both 16*S* rRNA and *mcrA* genes related to the anaerobic methane-oxidizing phylotype ANME-1 were found in cooler environments associated with hydrothermal flanges on the carbonate chimney and carbonate-lined fractures along the walls of the peridotite massif (Table 1).

Based on phylogenetic analyses, the eubacterial diversity associated with active carbonate samples from the LCHF was similarly high; sequences related to the Firmicutes were present at higher-temperature sites, and representatives of the Chloroflexi, epsilon, and gamma proteobacteria occurred within cooler environments (Table 1). The distribution of Firmicutes at the LCHF is especially intriguing given the physiological adaptations of this group to high temperature and high pH (*31*). Additionally, some species within the Firmicutes have been isolated from extreme environments and are capable of oxidizing hydrogen and reduced sulfur species. Therefore, they may play a critical role in the ecology of high-temperature environments at the LCHF. The bacterial sequences found at the LCHF included relatives of sulfur- and

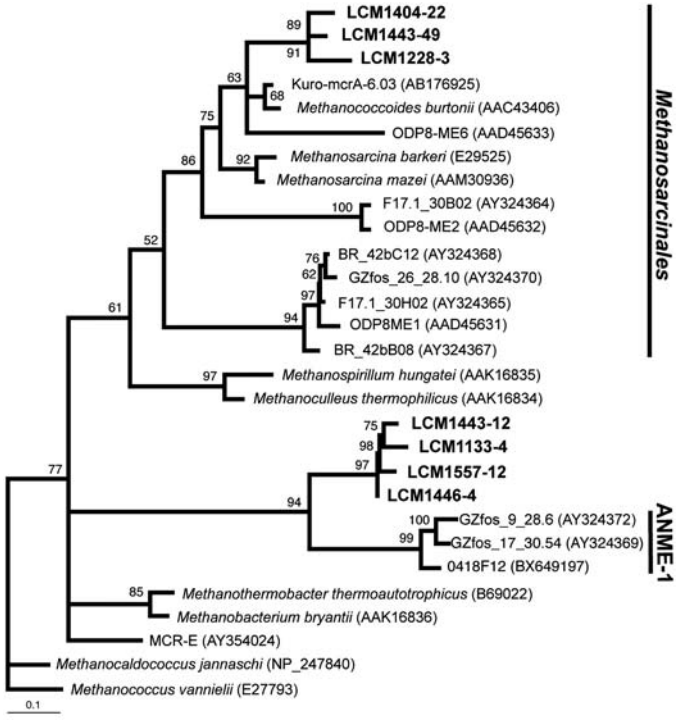

Fig. 6. Phylogenetic tree of partially sequenced *mcrA* clones isolated from carbonate samples relative to published sequences constructed with TREE-PUZZLE version 5.0 (*46*). Quartet-puzzling support values are shown at branch points; *Methanocaldococcus jannaschii* was used as the outgroup. LCM1404-22, LCM1443-49, LCM1443-12, and LCM1446-4 were isolated from marker C and LCM1228-3 from marker H, both of which are actively venting structures (see fig. S1 for locations). LCM1133-4 and LCM1557-12 were isolated from carbonate veins in serpentinite. GenBank Accession numbers for LCHF *mcrA* clones are AY760633 through AY760639. The scale bar represents 0.1 changes per nucleotide base.

Table 1. Biological Communities at Lost City.

Sample	*T* (°C)*	Microscopy				Phylogenetic analyses§									
		Cells (gww)†	FISH‡			Archaea			Eubacteria					*mcrA*	
			A	B	MS	MS	AN-1	MG1	γ	δ	ε	Fm	Cx	MS	AN-1
Poseidon															
Marker 2 (IMAX)flange	53–60	0.6 × 10^8 to 5.2 × 10^8	33	18	29	+			+		+	+	+		
Marker 3: top	59–75	0.02 × 10^8 to 1.3 × 10^8	41	12	33	+			+						
Marker C: flange and spire[e]	54–70	0.1 × 10^8 to 8.4 × 10^8	28	23	19	+	+		+	+	+		+	+	+
Beehive	91.4	5.8 × 10^6	21	8	18										
Other chimneys															
Marker 7: spire	24	<LOD = 4.7 × 10^8	22	24	17										
Marker H: spire and flange	17–67	0.03 × 10^8 to 3.1 × 10^8	19	38	10	+	+		+					+	
Peripheral (diffuse) regions	>7	0.1 × 10^8 to 4.8 × 10^8	8	29	5	+			+		+				
Near wall															
Spire on wall	>7	2.3 × 10^8 to 7.4 × 10^8	25	13	14										
Carbonate veins	>7	<LOD = 2.2 × 10^8	19	15	9		+		+		+				+
Extinct samples	Ambient	<LOD = 1.4 × 10^7	5	17	<1			+	+						

*Temperature (*T*) measured in situ either with *Alvin*'s temperature probe or with a sensor mounted on the hydrothermal fluid particulate sampler. †Number of organisms in gww; limit of detection (LOD) = ~ 10^4 cells gww. ‡Fluorescence in situ hybridization (FISH). FISH data are in % of total cell numbers. Abbreviations are as follows: A, Archaea; B, Eubacteria; MS, Lost City methanosarcinal phylotype. §Phylogenetic abbreviations are as follows: MS, Lost City methanosarcinal phylotype; AN-1, ANME-1; MGI, marine group 1 Crenarchaeota; γ, gamma proteobacteria; δ, delta proteobacteria; ε, epsilon proteobacteria; Fm, Firmicutes; Cx, Chloroflexi.

methane-oxidizing phylotypes and sulfate-reducing delta proteobacteria. The presence of distinct methane- and sulfur-cycling microbial communities at multiple temperature and environmental settings indicates a complex interaction between subseafloor geochemical processes at this site and chemolithotrophic microbial activity.

Structural and isotopic studies of lipid biomarkers in the LCHF samples document the presence of particular microbial lineages and the importance of specific metabolic processes. The carbonate vent structures contain up to 0.6 wt % total organic carbon (TOC), indicating a relatively high content of living and dead biomass within the vent structures. Abundances of $^{13}C_{TOC}$ varied widely from –3.1 to –18.1‰ (SOM text and table S1). Lipid extracts yielded abundant archaeal biomarkers consistent with results of the DNA analyses. The ether lipids archaeol, *sn*-2 and *sn*-3 hydroxyarchaeol, a putative dihydroxyarchaeol, and the hydrocarbon 2,6,10,15,19-pentamethylicosane (PMI), all found in the LCHF samples, have been linked to archaeal methanogens and methanotrophs (*32*, *33*). Less prevalent at the LCHF were biomarkers indicating the presence of eukaryotes (sterols) and bacteria (hopanoids). However, the presence at several vents of glycerol mono- and diethers with saturated and unsaturated C_{15} to C_{20} *n*-alkyl chains indicates that bacterial sulfate reduction may also be an active metabolic pathway. These data are also consistent with the observed strong negative correlation between concentrations of total sulfide and sulfate in LCHF vent fluids.

The archaeal populations are unusually enriched in ^{13}C. Values of $\delta^{13}C$ for TOC are positively correlated with the abundance of archaeal lipids. TOC from chimneys on the far eastern side of the field and from near the base of Poseidon is enriched in ^{13}C (δ = –4.6, -3.1‰ VPDB) and relatively rich in archaeal lipids, whereas a sample from a 91°C beehive structure on Poseidon has low concentrations of archaeal lipids and TOC with δ = –18.5‰. The causes of this trend can be examined by means of compound-specific isotopic analyses. The archaeal lipids discussed above have δ values ranging from –8.5 to +4.8‰ VPDB and they average –0.3‰. Glycerol mono- and diethers are similarly enriched in ^{13}C, whereas bacterial fatty acids are significantly depleted at –25‰. The isotopic composition of TOC must therefore represent a mass balance of isotopically distinct components.

The close association of archaea with sulfate-reducing bacteria that produce glycerol-ether lipids invites comparisons with microbial consortia operative at methane seeps (*33*, *34*). In seep environments, the two families of ether-linked lipids (archaeal and bacterial) have similar isotopic compositions. At the LCHF, the archaeal lipids are highly enriched in ^{13}C and are associated with relatively heavy $\delta^{13}C$ values of CH_4 in the vent fluids. The high H_2 concentrations, the occurrence of ^{13}C-enriched carbonate minerals (up to +13‰), and the abundance of ^{13}C-enriched archaeal lipids are all consistent with a role for H_2-consuming methanogens that use seawater DIC as a substrate and thus produce both CH_4 and biomass that is unusually enriched in ^{13}C. Therefore, in addition to an abiogenic origin of methane, produced by Fischer-Tropsch–type reactions involving H_2 and either mantle CO_2 or seawater bicarbonate, microbial activity is a viable source of CH_4 at Lost City. Given the wide variations in temperature and redox state, it is likely that further investigations will reveal a mosaic of processes, both abiotic and microbially catalyzed.

The highly sculpted large surface area of the Lost City structures provides ample space for faunal habitats, and many invertebrates were located within the porous channels and crevices of the carbonate. Actively venting carbonate habitats (~10° to 40°C) were dominated by several species of gastropods and amphipods, including *Bouvierella* affn. *curtirama*. The most abundant nonvent fauna were deep-sea euphausids and the amphipod *Primno evansi* (SOM text), which were probably attracted to the submersible lights during their diurnal vertical migrations. The hydrothermally active portions of friable flanges and spires were inhabited by numerous species of endemic polychaetes, nematodes, ostracods, stomatopods, and bivalves. Nonventing habitats less than a few meters away (such as the sides of inactive solidified carbonate structures, sedimented areas, and breccia cap rock) were dominated by nonendemic *Lophelia*, gorgonian, and *Desmophyllum* corals; galatheid crabs; turrid gastropods; foraminifera; pteropods; urchins; asteroids; ophiuroids; and typical deep-sea barnacles (such as *Poecilasma aurantia* and *Metaverruca inermis*). Thus, the boundary between vent and nonvent habitats is strongly demarcated at Lost City.

Initial in situ visual observations of the Lost City edifices suggested a notable absence of fauna (*4*), and even a cursory biomass comparison between the dominant Lost City fauna and Mid-Atlantic Ridge, East Pacific Rise, and Juan de Fuca vent fauna revealed significantly lower macrofaunal biomass at Lost City. The largest contributor to biomass at Lost City is the large mobile megafauna, including the wreckfish (*Polyprion americanus*), cut-throat eels (*Synaphobranchus kaupi*), and large geryonid crabs, which were all readily visible around active vents. The high-pH CH_4- and H_2-rich fluids are poor in the sulfide species that are typically relied on by vent faunal assemblages, and these factors may contribute to the relatively lower biomass observed at Lost City.

Despite the absence of readily observable fauna, the LCHF supports a species diversity that appears to be as high as that of any other known Mid-Atlantic Ridge vent site. Vent sites on the Mid-Atlantic Ridge typically host 30 to 50 macrofaunal species, with a total ~100 species residing within the eight major Mid-Atlantic Ridge sites (*35*, *36*). Initial analyses of >40 faunal samples recovered revealed that over 65 morpho-species representing 13 phyla are present. The majority (>90%) of these fauna were on the order of hundreds of micrometers or less in size. These were sampled via suction sampler from >10 active vent edifices and showed qualitative differences in species abundance and composition with substrate type.

Four morphospecies of gastropods were the most abundant fauna sampled from the carbonate. The most diverse group of invertebrates dominating the flange areas was polychaetes, including the families Dorvelleidae (including new species of *Ophiotrocha*), Ceratulidae, Glyceridae, Amphinomidae, and Polynoidae. A minimum of nine species were found, one-third of which are new. Current assessments of vent-dependent fauna within the Lost City field reveal that 58% of these fauna are endemic.

Implications. The range and complexity of environments hosting peridotites and other ultramafic rocks is vast. Under appropriate conditions, any of these might support hydrothermal systems similar to the LCHF. From ancient komatiitic rocks of the Early Archaean (*37*) to ophicalcite deposits within the Apennine ophiolites (*38*) comes evidence that hydrothermal systems have indeed been operative within ultramafic environments for much of Earth's history. Within the contemporary oceanic crust, there is a diverse array of submarine environments affected by ongoing serpentinization reactions, which include systems such as the Mariana forearc (*39*, *40*), the Arctic (*9*), the Antarctic (*10*), the Southwest Indian and Mid-Atlantic Ridge spreading networks (*41*, *42*), major transform faults (*17*, *43*), and highly extended rifted margins (*44*). Any of these tectonic settings could host LCHF-type ecosystems. Such systems may also have played a role in the origin and evolution of life on this planet and perhaps elsewhere (*45*).

References and Notes

1. F. N. Spiess *et al.*, *Science* **207**, 1421 (1980).
2. *The Subseafloor Biosphere at Mid-Ocean Ridges*, W. W. Wilcock, E. DeLong, D. S. Kelley, J. A. Baross, S. C. Cary, Eds. (Geophysical Monograph 144, American Geophysical Union, Washington, DC, 2004).
3. P. Michael, *Nature* **419**, 445 (2002).
4. D. S. Kelley *et al.*, *Nature* **412**, 145 (2001).
5. D. S. Kelley, G. L. Früh-Green, M. D. Lilley, in (*2*), pp. 167–189.
6. M. D. Lilley, D. A. Butterfield, J. A. Lupton, E. J. Olson, *Nature* **422**, 878 (2003).
7. Y. Lagabrielle, D. Bideau, M. Cannat, J. A. Karson, C. Mevel, in *Faulting and Magmatism at Mid-Ocean Ridges*, W. R. Buck, P. T. Delaney, J. A. Karson, Y. Lagabrielle, Eds. (Geophysical Monograph 106, Amer-

ican Geophysical Union, Washington, DC, 1998), pp. 153–176.
8. W. Bach, N. R. Banerjee, H. J. B. Dick, E. T. Baker, *Geochem. Geophys. Geosyst.* **3**, GC000279 (2001).
9. H. N. Edmonds *et al.*, *Nature* **421**, 252 (2003).
10. H. J. B. Dick, J. Lin, H. Schouten, *Nature* **426**, 405 (2003).
11. G. L. Früh-Green *et al.*, *Science* **302**, 495 (2003).
12. R. P. Lowell, P. A. Rona, *Geophys. Res. Lett.* **29**, 10.1029/2001GL01411 (2002).
13. T. L. Grove, S. W. Parman, *Earth Planet. Sci. Lett.* **219**, 173 (2004).
14. Materials and methods are available as supporting material on *Science* Online.
15. D. K. Blackman *et al.*, *Marine Geophsy. Res.* **23**, 443 (2004).
16. T. Schroeder, B. John, B. R. Frost, *Geology* **30**, 367 (2002).
17. J. A. Karson, in *Faulting and Magmatism at Mid-Ocean Ridges*, W. R. Buck, P. T. Delaney, J. A. Karson, Y. Lagabrielle, Eds. (Geophysical Monograph 106, American Geophysical Union, Washington, DC, 1998), pp. 177–218.
18. D. S. Kelley, J. A. Baross, J. R. Delaney, *Annu. Rev. Earth Planet. Sci.* **30**, 385 (2002).
19. J. L. Charlou, J. P. Donval, Y. Fouquet, P. Jean-Baptiste, N. Holm, *Chem. Geol.* **191**, 345 (2002).
20. D. R. Janecky, W. E. Seyfried Jr., *Geochim. Cosmochim. Acta* **50**, 1357 (1986).
21. C. Neal, G. Stanger, *Earth Planet. Sci. Lett.* **66**, 315 (1983).
22. M. E. Berndt, D. Allen, W. E. Seyfried Jr., *Geology* **24**, 351 (1996).
23. L. R. Wetzel, E. L. Shock, *J. Geophys. Res.* **105**, 8319 (2000).
24. T. M. McCollom, J. S. Seewald, *Geochim. Cosmochim. Acta* **65**, 3769 (2001).
25. M. D. Lilley *et al.*, *Nature* **364**, 45 (1993).
26. J. A. Welhan, H. Craig, *Eos* **60**, 863 (1979).
27. J. A. Welhan, H. Craig, in *Hydrothermal Processes at Seafloor Spreading Centers*, A. Rona Peter, K. Bostrom, L. Laubier, L. Smith Kenneth Jr., Eds. (Plenum, New York, 1983), pp. 391–409.
28. P. Fritz, I. D. Clark, J. C. Fontes, M. J. Whiticar, E. Faber, in *Proceedings of the 7th International Symposium on Water-Rock Interaction; Volume 1, Low Temperature Environments*, K. Kharaka Yousif, S. Maest Ann, Eds. (International Association of Geochemistry and Cosmochemistry and Alberta Research Council, Sub-Group on Water-Rock Interaction, Edmonton, Alberta, Canada, 1992), pp. 793–796.
29. T. A. Abrajano *et al.*, *Chem. Geol.* **71**, 211 (1988).
30. M. O. Schrenk, D. S. Kelley, S. A. Bolton, J. A. Baross, *Environ. Microbiol.* **6**, 1086 (2004).
31. A.-L. Reysenbach, D. Götz, D. Yernool, in *Biodiversity of Microbial Life*, J. T. Staley, A.-L. Reysenbach, Eds. (Wiley-Liss, New York, 2002), pp. 345–422.
32. J. M. Hayes, J. W. Valley, D. R. Cole, Eds., *Stable Isotope Geochemistry, Reviews in Mineralogy and Geochemistry* (Mineralogical Society of America, Washington, DC, 2001), vol. 43, chap. 3.
33. K. U. Hinrichs, R. E. Summons, V. Orphan, S. P. Sylva, J. M. Hayes, *Org. Geochem.* **31**, 1685 (2000).
34. V. Orphan *et al.*, *Proc. Natl. Acad. Sci. U.S.A.* **99**, 7663 (2002).
35. V. Tunnicliffe, C. M. R. Fowler, *Nature* **379**, 531 (1996).
36. A. V. Gebruk, S. V. Galkin, A. L. Vereshchaka, L. I. Moskalev, A. J. Southward, *Adv. Mar. Biol.* **32**, 93 (1997).
37. A. A. Suror, E. H. Arfa, *J. Afr. Earth Sci.* **24**, 315 (1997).
38. B. E. Treves, G. D. Harper, *Ofioliti* **19b**, 435 (1994).
39. M. M. Mottl, S. C. Komor, P. Fryer, C. L. Moyer, *Geochem. Geophys. Geosyst.* **4**, 11 (2003).
40. P. Fryer, C. G. Wheat, M. J. Mottl, *Geology* **27**, 103 (1997).
41. E. Gracia, J. L. Charlou, J. Radford-Knoery, L. Parson, *Earth Planet. Sci. Lett.* **177**, 89 (2000).
42. J. L. Charlou, J. P. Donval, Y. Fouquet, P. Jean-Baptiste, N. Holm, *Chem. Geol.* **191**, 345 (2002).
43. E. Bonatti, P. J. Michael, *Earth Planet. Sci. Lett.* **91**, 297 (1989).
44. T. J. Reston *et al.*, *Geology* **29**, 587 (2001).
45. E. L. Shock, M. D. Schulte, *J. Geophys. Res.* **103**, 28,513 (1998).
46. H. A. Schmidt, K. Strimmer, M. Vingron, A. von Haeseler, *Bioinformatics* **18**, 502 (2002).
47. We express our deep appreciation to the crews of the R/V *Atlantis* and *Alvin* for their support and help with the 2003 Lost City expedition. Their humor, friendship, and professionalism were instrumental to the success of the field program. We also very much appreciate the helpful comments of four anonymous reviewers. We thank B. Nelson for his time and help with the Sr analyses and for making his laboratory available to us, S. R. Emerson for guidance in chemical analyses of the carbonate samples and use of his laboratory facilities, and M. Lin for technical assistance with phylogenetic analyses. We acknowledge funding from NSF grants OCE0137206 (D.S.K.), OCE0136816 (J.A.K.), and OCE0136871 (D.R.Y. and T.M.S.). Work by J.A.B. was also supported by the NASA Astrobiology Institute through the Carnegie Geophysical Institute. Support to G.L.F.-G. was through Swiss National Science Foundation grant 2100-068055. J.M.H. was supported in part by the NASA Astrobiology Institute through the University of Rhode Island.

Supporting Online Material
www.sciencemag.org/cgi/content/full/307/5714/1428/DC1
Materials and Methods
SOM Text
Figs. S1 and S2
Table S1
References
Movies S1 and S2

9 July 2004; accepted 21 January 2005
10.1126/science.1102556

The Influence of *CCL3L1* Gene–Containing Segmental Duplications on HIV-1/AIDS Susceptibility

Enrique Gonzalez,[1]* Hemant Kulkarni,[1]* Hector Bolivar,[1]*† Andrea Mangano,[2]* Racquel Sanchez,[1]‡ Gabriel Catano,[1]‡ Robert J. Nibbs,[3]‡ Barry I. Freedman,[4]‡ Marlon P. Quinones,[1]‡ Michael J. Bamshad,[5] Krishna K. Murthy,[6] Brad H. Rovin,[7] William Bradley,[8,9] Robert A. Clark,[1] Stephanie A. Anderson,[8,9] Robert J. O'Connell,[9,10] Brian K. Agan,[9,10] Seema S. Ahuja,[1] Rosa Bologna,[11] Luisa Sen,[2] Matthew J. Dolan,[9,10,12]§ Sunil K. Ahuja[1]§

Segmental duplications in the human genome are selectively enriched for genes involved in immunity, although the phenotypic consequences for host defense are unknown. We show that there are significant interindividual and interpopulation differences in the copy number of a segmental duplication encompassing the gene encoding CCL3L1 (MIP-1αP), a potent human immunodeficiency virus–1 (HIV-1)–suppressive chemokine and ligand for the HIV coreceptor CCR5. Possession of a *CCL3L1* copy number lower than the population average is associated with markedly enhanced HIV/acquired immunodeficiency syndrome (AIDS) susceptibility. This susceptibility is even greater in individuals who also possess disease-accelerating *CCR5* genotypes. This relationship between *CCL3L1* dose and altered HIV/AIDS susceptibility points to a central role for CCL3L1 in HIV/AIDS pathogenesis and indicates that differences in the dose of immune response genes may constitute a genetic basis for variable responses to infectious diseases.

Duplicated host defense genes that are known to have dosage effects are thought to contribute to the genetic basis of some complex diseases, although direct evidence for this is lacking. We surmised that a hotspot for segmental duplications on human chromosome 17q might be relevant to immunity against infectious diseases such as HIV-1 because it encompasses two CC chemokine genes, CC chemokine ligand 3-like 1 (*CCL3L1*; other names, *MIP-1αP* and *LD78*β) and *CCL4L1* (*MIP-1*β*-like*), which represent the duplicated isoforms of the genes encoding CCL3 and CCL4, respectively (*1*–*3*). As a consequence of these duplications, the copy number of *CCL3L1* and *CCL4L1* varies among individuals (*2*, *3*) (fig. S1A). This is important because CCL3L1 is the most potent known ligand for CC chemokine receptor 5 (CCR5), the major coreceptor for HIV, and it is a dominant HIV-suppressive chemokine (*3*).

In light of this relationship between CCL3L1 and its in vitro effect on HIV infection, we selected HIV infection as a model system in which to test our hypothesis that segmental duplications causing dosage effects of host defense genes are associated with phenotypic effects in vivo. To test this hypothesis, we determined the distribution of chemokine gene–containing segmental duplications in 1064 humans from 57 populations and 83 chimpanzees (*4*). We next analyzed 4308 HIV-1–positive (HIV^+) and HIV-1–negative (HIV^-) individuals from groups with different geographical ancestries (e.g., Africans and Europeans) to determine if the risk of acquiring HIV and the rate at which HIV disease progressed were sensitive to differences in the dose of *CCL3L1*

A Serpentinite-Hosted Ecosystem: The Lost City Hydrothermal Field

Deborah S. Kelley, Jeffrey A. Karson, Gretchen L. Früh-Green, Dana R. Yoerger, Timothy M. Shank, David A. Butterfield, John M. Hayes, Matthew O. Schrenk, Eric J. Olson, Giora Proskurowski, Mike Jakuba, Al Bradley, Ben Larson, Kristin Ludwig, Deborah Glickson, Kate Buckman, Alexander S. Bradley, William J. Brazelton, Kevin Roe, Mitch J. Elend, Adélie Delacour, Stefano M. Bernasconi, Marvin D. Lilley, John A. Baross, Roger E. Summons and Sean P. Sylva

Science **307** (5714), 1428-1434.
DOI: 10.1126/science.1102556